



**HAL**  
open science

## **A bifunctional sea anemone peptide with Kunitz type protease and potassium channel inhibiting properties.**

Steve Peigneur, Bert Billen, Rita Derua, Etienne Waelkens, Sarah Debaveye, László Béress, Jan Tytgat

### ► **To cite this version:**

Steve Peigneur, Bert Billen, Rita Derua, Etienne Waelkens, Sarah Debaveye, et al.. A bifunctional sea anemone peptide with Kunitz type protease and potassium channel inhibiting properties.. *Biochemical Pharmacology*, 2011, 82 (1), pp.81. 10.1016/j.bcp.2011.03.023 . hal-00701259

**HAL Id: hal-00701259**

**<https://hal.science/hal-00701259>**

Submitted on 25 May 2012

**HAL** is a multi-disciplinary open access archive for the deposit and dissemination of scientific research documents, whether they are published or not. The documents may come from teaching and research institutions in France or abroad, or from public or private research centers.

L'archive ouverte pluridisciplinaire **HAL**, est destinée au dépôt et à la diffusion de documents scientifiques de niveau recherche, publiés ou non, émanant des établissements d'enseignement et de recherche français ou étrangers, des laboratoires publics ou privés.

## Accepted Manuscript

Title: A bifunctional sea anemone peptide with Kunitz type protease and potassium channel inhibiting properties.

Authors: Steve Peigneur, Bert Billen, Rita Derua, Etienne Waelkens, Sarah Debaveye, László Béress, Jan Tytgat



PII: S0006-2952(11)00210-3  
DOI: doi:10.1016/j.bcp.2011.03.023  
Reference: BCP 10863

To appear in: *BCP*

Received date: 10-2-2011  
Revised date: 24-3-2011  
Accepted date: 25-3-2011

Please cite this article as: Peigneur S, Billen B, Derua R, Waelkens E, Debaveye S, Béress L, Tytgat J, A bifunctional sea anemone peptide with Kunitz type protease and potassium channel inhibiting properties., *Biochemical Pharmacology* (2008), doi:10.1016/j.bcp.2011.03.023

This is a PDF file of an unedited manuscript that has been accepted for publication. As a service to our customers we are providing this early version of the manuscript. The manuscript will undergo copyediting, typesetting, and review of the resulting proof before it is published in its final form. Please note that during the production process errors may be discovered which could affect the content, and all legal disclaimers that apply to the journal pertain.

## A BIFUNCTIONAL SEA ANEMONE PEPTIDE WITH KUNITZ TYPE PROTEASE AND POTASSIUM CHANNEL INHIBITING PROPERTIES.

Steve Peigneur<sup>1</sup>, Bert Billen<sup>1</sup>, Rita Derua<sup>2</sup>, Etienne Waelkens<sup>2</sup>, Sarah Debaveye<sup>1</sup>,  
László Béress<sup>3</sup>, Jan Tytgat<sup>1§</sup>

From the <sup>1</sup>Laboratory of Toxicology, University of Leuven (K.U. Leuven), Campus Gasthuisberg O&N2, Herestraat 49, P.O. Box 922, B-3000 Leuven, Belgium, <sup>2</sup>Laboratory of Protein Phosphorylation and Proteomics, University of Leuven, <sup>3</sup> Clinic for Immunology and Rheumatology, Research group Experimental Peptide chemistry, medical High School Hanover, Germany

§ To whom correspondence should be addressed. Tel.: +32 1632 34 03; Fax: +32 16 32 34 05; E-mail: [jan.tytgat@pharm.kuleuven.be](mailto:jan.tytgat@pharm.kuleuven.be)

**Abstract** Sea anemone venom is a known source of interesting bioactive compounds, including peptide toxins which are invaluable tools for studying structure and function of voltage-gated potassium channels. APEKTx1 is a novel peptide isolated from the sea anemone *Anthopleura elegantissima*, containing 63 amino acids cross-linked by 3 disulfide bridges. Sequence alignment reveals that APEKTx1 is a new member of the type 2 sea anemone peptides targeting voltage-gated potassium channels (K<sub>V</sub>'s), which also include the kalicludines from *Anemonia sulcata*. Similar to the kalicludines, APEKTx1 shares structural homology with both the basic pancreatic trypsin inhibitor (BPTI), a very potent Kunitz-type protease inhibitor, and dendrotoxins which are powerful blockers of voltage-gated potassium channels. In this study, APEKTx1 has been subjected to a screening on a wide range of 23 ion channels expressed in *Xenopus laevis* oocytes: 13 cloned voltage-gated potassium channels (K<sub>V</sub>1.1-K<sub>V</sub>1.6, K<sub>V</sub>1.1 triple mutant, K<sub>V</sub>2.1, K<sub>V</sub>3.1, K<sub>V</sub>4.2, K<sub>V</sub>4.3, hERG, the insect channel *Shaker* IR), 2 cloned hyperpolarization-activated cyclic nucleotide-sensitive cation non-selective channels (HCN1 and HCN2) and 8 cloned voltage-gated sodium channels (Na<sub>V</sub>1.2-Na<sub>V</sub>1.8 and the insect channel DmNa<sub>V</sub>1). Our data shows that APEKTx1 selectively blocks K<sub>V</sub>1.1 channels in a very potent manner with an IC<sub>50</sub> value of 0.9 nM. Furthermore, we compared the trypsin inhibitory activity of this toxin with BPTI. APEKTx1 inhibits trypsin with a dissociation constant of 124 nM. In conclusion, this study demonstrates that APEKTx1 has the unique feature to combine the dual functionality of a potent and selective blocker of K<sub>V</sub>1.1 channels with that of a competitive inhibitor of trypsin.

**Keywords** *Anthopleura elegantissima* · K<sub>V</sub> channel inhibitor · sea anemone toxin · protease inhibitor ·

### 1. Introduction

Among ion channels, potassium channels are the most diverse class of ion channels and they are key determinants of neuronal excitability. They regulate a variety of cellular processes and functions such as heart rate, neurotransmitter release and nerve conduction, insulin secretion, blood pressure and muscle contraction [1,2]. In the mammalian genome more than 100 genes are encoding the pore forming  $\alpha$  subunits and auxiliary  $\beta$  subunits of K<sup>+</sup> channels. Together with these numerous genes, the presence of spliced variants, association with chaperone and scaffolding molecules and the formation of heteromultimeric channels contribute greatly to the diversity of the K<sup>+</sup> channel family [2]. This family has been divided into 15 subfamilies of which the voltage gated potassium channels (K<sub>V</sub>) represent one of these subfamilies [3]. They determine neuronal intrinsic electrical excitability by repolarization of the membrane after initiation of the action potential [4]. Upon depolarization of the membrane, K<sub>V</sub> channels will open within 1 ms, allowing the flux of K<sup>+</sup> ions driven by their electrochemical gradient [1,2]. Functional K<sub>V</sub> channels are formed by a complex of four pore forming  $\alpha$  subunits associated with one or

1  
2  
3  
4 more auxiliary  $\beta$  subunits. Each  $\alpha$  subunit consists of six transmembrane spanning segments (S1-S6). The  
5 first four transmembrane segments form the voltage sensing domain with S4 serving as the voltage  
6 sensor. This S4 segment has been modeled using the crystal structure of the bacterial  $K_v$  channel  $K_vAP$   
7 and contains 4 conserved Arg residues. These positively charged basic residues display a net movement  
8 outwards upon depolarization allowing conformational changes resulting in the opening of the pore [5,6].  
9 The pore region of the channels is formed by the S5 and S6 segments which are connected by a re-entrant  
10 P-loop. The P-loop contains an extremely well conserved domain among the  $K_v$  channels, the so-called  
11 signature sequence (-TXGYGD-) and comprises the selectivity filter, the pore helix and the turret region  
12 [7]. The auxiliary  $\beta$  subunits of  $K_v$  channels ( $K_v\beta$ ) are cytoplasmic proteins, capable of modifying  $K_v$   
13 channel biophysical properties.  
14

15 Since the beginning of last century sea anemones have been studied with an increasing interest. Although  
16 a number of sea anemone toxins have been isolated and characterized, these animals remain poorly  
17 studied in comparison with other venomous animals such as scorpions, spiders, cone snails or snakes. Sea  
18 anemones are a known pharmacological treasure of biological active compounds acting upon a diverse  
19 panel of ion channels such as TRPV1, voltage-gated sodium and potassium channels [8-11]. Of these  
20 different toxins those that target sodium channels are the best studied group with more than 100 known  
21 toxins [12]. In contrast, no more than 12 potassium channel toxins have been characterized to date. Based  
22 on structural differences and activity profile, these potassium channel toxins can be divided into 4  
23 structural classes [11,13-15]. Up to date 6 toxins from *A. elegantissima* have been isolated and  
24 characterized: APE1-1, APE1-2, APE2-2 and ApC which are type 1 sodium channel toxins; APETx1 a  
25 selective modifier of the human ether a go-go related gene  $K^+$  channel (hERG) and APETx2 which  
26 specifically inhibits the Acid Sensing Ion Channel (ASIC3) [15-18]. In this work we present the  
27 purification, biochemical analysis and electrophysiological characterization of a very potent and selective  
28  $K_v1.1$  blocker which represents the newest member of the sea anemone type 2 potassium channel toxins.  
29  
30

## 31 32 **2. Material and methods**

### 33 34 2.1. Toxin purification.

35  
36 The toxin APEKTx1 was purified as described previously [16,17,19]. The fraction containing APEKTx1  
37 was further purified by RP-HPLC with a semi preparative Vydac C18 column (4.6X250 mm). Solvent  
38 A was 0.1% TFA in water, solvent B was 0.085% TFA in acetonitrile. A linear gradient from 0 to 80%  
39 solution B was developed for 80 min at a flow rate of 1ml/min. A second purification was performed in  
40 the same conditions as described above. All final fractions were dried by speed-vac evaporation and  
41 stored at  $-20^\circ\text{C}$ .  
42  
43

### 44 45 2.2. Biochemical characterization of toxins.

46  
47 The mass of the intact toxin was measured by MALDI-TOF (4800 Analyzer, Applied Biosystems, USA)  
48 as well as by ESI-QUAD analysis (4000QTRAP, Applied Biosystems, USA).

49 The toxin peptide was subjected to Edman degradation on an Applied Biosystems Procise instrument. The  
50 toxin was digested with legumain (R&D Systems, USA). A MALDI TOF/TOF instrument (4800  
51 Analyzer, Applied Biosystems, USA) was used for *de novo* sequencing analysis of the obtained  
52 fragments. These fragments were subjected to MS/MS analysis and the spectra were manually interpreted.  
53

### 54 55 2.3. Expression of voltage-gated ion channels in *Xenopus laevis* oocytes.

56  
57 For the expression of the VGPCs (r $K_v1.1$  (Accession number: NM173095), r $K_v1.2$  (NM012970), h $K_v1.3$   
58 (L23499), r $K_v1.4$  (NM012971), r $K_v1.5$  (NM012972), r $K_v1.6$  (NM575671), Shaker IR (CG12348),  
59 r $K_v2.1$  (NM013186), h $K_v3.1$  (NM004976), r $K_v4.2$  (NM031730), r $K_v4.3$  (NM031739), hERG  
60 (NM000238), mHCN 1 (NM010408), mHCN 2 (NM008226) and the VGSCs (r $Na_v1.2$  (NM012647),  
61  
62  
63  
64  
65

1  
2  
3  
4 rNa<sub>v</sub>1.3 (NM012647), rNa<sub>v</sub>1.4 (M26643), hNa<sub>v</sub>1.5 (NM198056), mNa<sub>v</sub>1.6 (L39018), rNa<sub>v</sub>1.7  
5 (AF000368), rNa<sub>v</sub>1.8 (NM017247), rβ1 (NM017288), hβ1 (NM001037) and the insect channel DmNa<sub>v</sub>1  
6 (NC004354) in *Xenopus* oocytes, the linearized plasmids were transcribed using the T7 or SP6  
7 mMESSAGE-mMACHINE transcription kit (Ambion, USA). The harvesting of stage V-VI oocytes from  
8 anaesthetized female *Xenopus laevis* frog was previously described [20]. Oocytes were injected with 50 nl  
9 of cRNA at a concentration of 1 ng/nl using a micro-injector (Drummond Scientific, USA). The oocytes  
10 were incubated in a solution containing (in mM): NaCl, 96; KCl, 2; CaCl<sub>2</sub>, 1.8; MgCl<sub>2</sub>, 2 and HEPES, 5  
11 (pH 7.4), supplemented with 50 mg/l gentamycin sulfate.

#### 14 2.4. Electrophysiological recordings.

16 Two-electrode voltage-clamp recordings were performed at room temperature (18-22°C) using a  
17 Geneclamp 500 amplifier (Molecular Devices, USA) controlled by a pClamp data acquisition system  
18 (Axon Instruments, USA). Whole cell currents from oocytes were recorded 1-4 days after injection. Bath  
19 solution composition was ND96 (in mM): NaCl, 96; KCl, 2; CaCl<sub>2</sub>, 1.8; MgCl<sub>2</sub>, 2 and HEPES, 5 (pH 7.4)  
20 or HK (in mM): NaCl, 2; KCl, 96; CaCl<sub>2</sub>, 1.8; MgCl<sub>2</sub>, 2 and HEPES, 5 (pH 7.4). Voltage and current  
21 electrodes were filled with 3M KCl. Resistances of both electrodes were kept between 0.5-1.5 MΩ. The  
22 elicited currents were filtered at 1 kHz and sampled at 0.5 kHz (for potassium currents) or at 20 kHz (for  
23 sodium currents) using a four-pole low-pass Bessel filter. Leak subtraction was performed using a -P/4  
24 protocol. K<sub>v</sub>1.1-K<sub>v</sub>1.6 and *Shaker* currents were evoked by 500 ms depolarizations to 0 mV followed by  
25 a 500 ms pulse to -50 mV, from a holding potential of -90 mV. Current traces of hERG channels were  
26 elicited by applying a +40 mV prepulse for 2 s followed by a step to -120 mV for 2 s. K<sub>v</sub>2.1, K<sub>v</sub>3.1 and  
27 K<sub>v</sub>4.2, K<sub>v</sub>4.3 currents were elicited by 500 ms pulses to +20mV from a holding potential of -90 mV.  
28 Sodium current traces were, from a holding potential of -90 mV, evoked by 100 ms depolarizations to V<sub>max</sub>  
29 (the voltage corresponding to maximal sodium current in control conditions). In order to investigate the  
30 current-voltage relationship, current traces were evoked by 10 mV depolarization steps from a holding  
31 potential of -90 mV. g<sub>v</sub> curves were calculated from IV relationships as follows:  $g_K = I_K / (E_m - E_K)$  with  
32  $E_K = (RT/zF) \ln([K^+]_o/[K^+]_i)$ . In these equations g<sub>K</sub> represents the conductance, I<sub>K</sub> the potassium current,  
33 E<sub>m</sub> the membrane potential, E<sub>K</sub> the reversal potential, R the gas constant (8.31 J/K.mol), T the  
34 temperature, z the charge of the ion (for K<sup>+</sup> ions: z = 1), F the Faraday's constant (96.500 C/mol), [K<sup>+</sup>]<sub>o</sub>  
35 and [K<sup>+</sup>]<sub>i</sub> respectively are the extracellular and intracellular K<sup>+</sup> ion concentrations. The values of I<sub>K</sub> or g<sub>K</sub>  
36 were plotted as function of voltage and fitted using the Boltzmann equation:  $g_K/g_{max} = [1 + (\exp(Vg - V)/k)]^{-1}$ ,  
37 where g<sub>max</sub> represents maximal g<sub>K</sub>, Vg is the voltage corresponding to half-maximal conductance,  
38 and k is the slope factor. To assess the concentration dependency of the APEKTx1 induced inhibitory  
39 effects, a concentration-response curve was constructed, in which the percentage of current inhibition was  
40 plotted as a function of toxin concentration. Data were fitted with the Hill equation:  $y = 100/[1 + (IC_{50}/[toxin])^h]$ ,  
41 where y is the amplitude of the toxin-induced effect, IC<sub>50</sub> is the toxin concentration at half-maximal efficacy,  
42 [toxin] is the toxin concentration, and h is the Hill coefficient. To investigate the bimolecular kinetics of  
43 toxin inhibition, oocytes expressing wild type K<sub>v</sub>1.1 channels were depolarized to 0 mV for 0.5 s from a  
44 holding potential of -90 mV every 5 s, both in the absence and presence of different concentrations of toxin.  
45 The obtained current values were plotted as a function of time. Data were fitted with the following  
46 exponential equation:  $y = Ae^{-t/\tau}$ , where t represents the time, A is the amplitude of the current and τ is  
47 the time constant for toxin binding (τ<sub>on</sub>) or toxin unbinding (τ<sub>off</sub>). The first-order association rate constant  
48 (k<sub>on</sub>) was calculated using following equation:  $\tau_{on} = (k_{on} + k_{off})^{-1}$ . The first-order dissociation  
49 constant (k<sub>off</sub>) was calculated using the equation:  $\tau_{off} = k_{off}^{-1}$ . Comparison of two sample means  
50 was made using a paired Student's t test (p < 0.05). All data represent at least 3 independent experiments  
51 (n ≥ 3) and are presented as mean ± standard error.

#### 57 2.5. Kunitz-type inhibition activity.

1  
2  
3  
4 The possible trypsin inhibition activity of APEKTx1 was measured spectrophotometrically as described  
5 previously [21]. Briefly, aliquots containing a final concentration of 3  $\mu$ M trypsin (from bovine pancreas,  
6 TPCK treated, Sigma-Aldrich, USA) were incubated with various concentrations of peptides in 5 mM  
7  $\text{CaCl}_2$  and 50 nM Tris-HCl, pH 7.8. After incubation for 3 h at 25°C the remaining trypsin activity was  
8 determined by addition of 5  $\mu$ l of a 5 mM  $\text{N}\alpha$ -benzoyl-DL-arginine p-nitroanilide (BAPNA, Sigma-  
9 Aldrich,USA). Paranitroaniline release was measured at 405 nm.

## 10 11 12 2.6. Molecular modeling.

13  
14 APEKTx1 was modeled using the publicly available program MODELLER9v8  
15 (<http://www.salilab.org/modeller>) using textilin-1, a Kunitz-type serine protease inhibitor from the  
16 venom of the Australian common brown snake *Pseudonaja textilis* (PDB code 3BYB;  
17 <http://www.pdb.org/pdb>) as template.

## 18 19 20 3. Results

### 21 22 3.1. Purification of APEKTx1.

23  
24 The screening of fractions obtained from the sea anemone *A. elegantissima*, after anion and cation  
25 exchange and gel filtration, yielded one fraction which was able to fully block  $\text{K}_v1.1$  channels. This  
26 fraction was further purified in 2 steps using reversed-phase HPLC. A linear gradient from 0 to 80%  
27 solution B was developed for 80 min at a flow rate of 1ml/min. A second purification was performed in  
28 the same conditions as described above (fig.1).

### 29 30 31 3.2. Biochemical properties.

32  
33 With MALDI analysis in the linear mode, a broad mass peak with an apex mass of 7468.8 Da was  
34 measured. This experimental mass of 7475 Da corresponds well with the theoretical mass of 7468.5 Da.  
35 During ESI analysis, a mass of 7484.8 Da was observed, suggesting an oxidation of Met32. The intact  
36 toxin was subjected to Edman degradation. Since only the 20 first N-terminal amino acids could be  
37 reliably sequenced, we subjected the toxin to a proteolytic treatment in order to obtain fragments  
38 amenable to *de novo* sequencing analysis by MALDI TOF/TOF instrument. Digestion of the toxin by  
39 trypsin, gluC, thermolysin turned out to be unsuccessful. Finally, an asparaginylendopeptidase was found  
40 to cut the toxin peptide into smaller fragments. The digestion was executed according to the protocol of  
41 the manufacturer. After digestion, the resulting peptides were separated and desalted by HPLC. The  
42 HPLC fractions were dried by speed-vac evaporation and resolubilized in alfa-cyano 4-hydrocinnamic  
43 acid matrix solution before analysis by MALDI TOF/TOF. The protein sequence data reported in this  
44 paper will appear in the UniProt Knowledgebase under the accession number P86862.

### 45 46 47 48 3.3. Electrophysiological experiments.

49  
50 Sequence alignment (fig. 2A) indicated that APEKTx1 is a new member of the type 2 sea anemone  
51 peptides directing against voltage-gated potassium channels, which also include the kalicludines from *A.*  
52 *sulcata* and SHTX II from *Stichodactyla haddoni* [21,22]. From figure 2B it can be seen that APEKTx1  
53 also shares homology with protease inhibitors from other sea anemones and with the potent Kunitz-type  
54 protease inhibitor Bovine Pancreatic Trypsin Inhibitor (BPTI). Previous electrophysiological experiments  
55 in *Xenopus laevis* oocytes have shown that the kalicludines block  $\text{K}_v1.2$  channels with  $\text{IC}_{50}$  values around  
56 1  $\mu$ M. SHTX II was reported to inhibit the binding of  $^{125}\text{I}$ - $\alpha$ -DTX to synaptosomal membranes with an  $\text{K}_d$   
57 value of 650 nM [21,22]. As shown in figure 3A, the pure peptide APEKTx1 was subject of a wide  
58 screening on 23 ion channels: 12 cloned voltage-gated potassium channels ( $\text{K}_v1.1$ - $\text{K}_v1.6$ ,  $\text{K}_v1.1$  mutant,  
59  $\text{K}_v2.1$ ,  $\text{K}_v3.1$ ,  $\text{K}_v4.2$ ,  $\text{K}_v4.3$ , hERG, the insect channel Shaker IR); 2 cloned hyperpolarization-activated  
60  
61  
62  
63  
64  
65

1  
2  
3  
4 cyclic nucleotide-sensitive cation non-selective channels (HCN1 and HCN2) and 8 cloned voltage-gated  
5 sodium channels ( $\text{Na}_v1.2$ - $\text{Na}_v1.8$  and the insect channel  $\text{DmNa}_v1$ ). Surprisingly, at concentrations up to 1  
6  $\mu\text{M}$ , no significant effect could be observed on the other ion channel isoforms tested. Figure 3B shows  
7 original traces for wild type  $\text{K}_v1.1$  channels with application of 0.3, 1 and 3 nM APEKTx1 and for mutant  
8  $\text{K}_v1.1$  channels with application of 100  $\mu\text{M}$  APEKTx1. A concentration response curve was constructed  
9 in order to determine the concentration at which half of the channels were blocked by APEKTx1. The  
10  $\text{IC}_{50}$  value yielded  $0.9 \pm 0.1$  nM (fig. 4A). Thus APEKTx1 inhibits  $\text{K}_v1.1$  channels with the same potency  
11 as DTX I and  $\alpha$ -DTX and is approximately 700 to 3000 times more potent than other known 2 sea  
12 anemone peptides directed against  $\text{K}_v$  channels. Moreover, this also means that at concentrations which  
13 are a 1000-fold the  $\text{IC}_{50}$  value of APETx1 on  $\text{K}_v1.1$ , this toxin still discriminates between subtype  
14 isoforms.

15  
16 The inhibition of  $\text{K}_v1.1$  channels by APEKTx1 was not voltage-dependent as in a range of test potentials  
17 from -30 mV to +40 mV no difference in the degree of APEKTx1 induced block could be observed (n=8)  
18 (fig. 4B).

19  
20 In order to investigate if the observed current inhibition is due to pore blockage or rather to altered  
21 channel gating upon APEKTx1 binding, the  $IV$  and  $gV$  curves in ND96 and HK solution were constructed  
22 (fig. 4C and D). Application of 10 nM APEKTx1 caused  $80.45 \pm 2.23\%$  and  $84.21 \pm 3.74\%$  inhibition of  
23 the potassium current in ND96 and HK, respectively (n=10). In ND96, the  $g_{max}$  curve in control and in the  
24 presence of 10 nM toxin was characterized by a  $V_{1/2}$  value of  $-15.7 \pm 1.23$  mV and  $-12.71 \pm 0.5$  mV (n=8)  
25 respectively. In HK, the  $V_{1/2}$  was respectively,  $-25.84 \pm 2.53$  mV and  $-19.89 \pm 3.2$  mV (n=8). It can be  
26 concluded that in both solutions no significant difference in  $V_{1/2}$  values occurred ( $P>0.05$ ). Furthermore,  
27 the  $IV$  relationship in HK solution shows that the reversal potential,  $E_K$  is not significantly influenced by  
28 APEKTx1 ( $P>0.05$ ; n=8).  $E_K$  values yielded  $-7.56 \pm 2.45$  mV in control and  $-7.96 \pm 1.92$  mV after  
29 application of toxin. All together, these experiments imply that current inhibition upon APEKTx1 binding  
30 does not result from changes in the voltage-dependence of channel gating. Presumably, APEKTx1 acts by  
31 blocking the pore in the open state of the  $\text{K}_v$  channel.

32  
33 Blockage of  $\text{K}_v1.1$  channels occurred rapidly and its binding was reversible since the current recovered  
34 quickly and completely upon washout (n=10) (fig. 4E). Both characteristics suggest an extracellular site  
35 of action. The reversibility of current inhibition is in contrast with DTX K binding. Toxin K binding is  
36 reversible at low concentrations but becomes irreversibly at concentrations higher than its  $\text{IC}_{50}$  value.  
37 However, alanine substitution of the Lys3 or Lys26 rendered DTX K binding reversible, possibly  
38 explaining the reversible binding of APEKTx1 since this toxin also possess neutral residues at these  
39 positions. Another observed difference between both toxins is that DTX K cannot fully inhibit the  
40 potassium current, even at very high concentrations. APEKTx1 however, is able to completely inhibit the  
41 current.

42  
43 Because APEKTx1 did not alter channel gating and binding was reversible we investigated whether  
44 APEKTx1 blockage followed the kinetic behavior of a bimolecular reaction [23]. Figure 4F shows the  
45 effects of increasing concentrations APEKTx1 on a  $\text{K}_v1.1$  channel. The apparent first order association  
46 rate constant  $k_{on}$  (open circles) increased linearly with toxin concentration, while the second order  
47 dissociation constant  $k_{off}$  (closed circles) remained constant. Both values are in concordance with the  
48 scheme of a bimolecular reaction. The influence on toxin-channel binding by through-space electrostatic  
49 forces between charged residues of the  $\text{K}_v1.1$  channel and of APEKTx1 was also examined. This was  
50 done by measuring the effectiveness of APEKTx1 binding on  $\text{K}_v1.1$  channels in solutions of different  
51 ionic strength. As described above, the  $\text{IC}_{50}$  value of APEKTx1 for  $\text{K}_v1.1$  homomeric channels was  $0.9 \pm$   
52  $0.1$  nM. However, when using an iso-osmotic solution with a 48 mM NaCl concentration (sucrose  
53 substitution) the obtained  $\text{IC}_{50}$  value was  $0.43 \pm 0.07$  nM. This 2 fold increase in APEKTx1 potency  
54 underlines that through-space electrostatic interaction is involved in APEKTx1 binding. These results are  
55 in corroboration with previously described similar observations for charybdotoxin binding to Shaker  
56 channels and for  $\alpha$ -DTX binding to  $\text{K}_v1.1$  channels [23-25].

57  
58 In order to define the  $\alpha$ -dendrotoxin footprint on mammalian potassium channels, 3 mutations (A352P,  
59 E353S and Y379H) were introduced in the dendrotoxin binding site, located in the H5 loop between the  
60  
61  
62  
63  
64  
65

transmembrane domains S5 and S6 of  $K_v1.1$  subunits (fig. 5). By mutating these 3 particular residues, the pore region of the  $K_v1.1$  triple mutant closely resembles this one of  $K_v1.3$  channels [23,24]. We investigated whether the sensitivity of APEKTx1 for  $K_v1.1$  could be affected by mutating these 3 critical residues. Interestingly, even at extreme high concentrations, APEKTx1 was unable to induce full blockage of current through these mutated  $K_v1.1$  channels. Application of 100  $\mu$ M APEKTx1 caused only 53 % inhibition (n=4) and the obtained  $IC_{50}$  yielded  $10.8 \pm 0.6 \mu$ M (fig. 4 A and Fig. 3B). This dramatic loss of affinity underlines the crucial interaction of these mutated residues with the toxin. Since it was reported that DTX K only needs one  $K_v1.1$  subunit to cause inhibition of the potassium current through wild type heteromultimeric channels [26], we investigated also if DTX K could block the triple mutant. Concentration response curves were constructed for both  $K_v1.1$  wild type and triple mutant channels (fig. 4A). The observed  $IC_{50}$  value for wild type channels was  $0.51 \pm 0.064$  nM which is in good accordance with previous reported values [27]. For mutant channels the  $IC_{50}$  was  $5.28 \pm 0.23$  nM. This means a 10-fold decrease in sensitivity compared to wild type channels.

### 3.4. Trypsin inhibition activity.

As all members of the type 2 sea anemone toxins APEKTx1 share sequence homology with the well characterized and potent Kunitz-type protease inhibitor BPTI, we also investigated if APEKTx1 could block trypsin activity. In order to do this, trypsin was incubated with different concentrations of APEKTx1 at room temperature for 3 hours to reach equilibrium. In the same conditions, trypsin was also incubated with DTX I, DTX K or BPTI. The protease inhibition activity was determined spectrophotometrically after incubation by measuring the ability of the remaining free trypsin to release paranitroaniline from BAPNA. It has been shown before that the kalicludines have a very similar inhibition profile as BPTI [21]. Figure 6 shows that APEKTx1 is a trypsin inhibitor with a  $K_d = 124$  nM. Presumably, APEKTx1 is a competitive trypsin inhibitor. A 3-fold molecular excess of APEKTx1 over trypsin completely inhibited the paranitroaniline release. However, this is almost 3 times the amount of BPTI or the kalicludines necessary to reach total inhibition of trypsin activity. The same figure also indicates that DTX I and DTX K, could not inhibit the trypsin activity, even at a 6:1 ratio of toxin over trypsin.

## 4. Discussion

The unique feature of a dual functionality within one molecule is intriguing. However, since the production of toxins is an energy demanding task for an organism, the dual effects contained within one molecule can be seen as an efficient and economic manner to save energy with a maximal pharmacological output. Furthermore, the dual effect has clearly advantages for the sea anemone in both an offensive and defensive point of view: the presence of a trypsin inhibitor will prolong the half-life of the peptides in the venom and therefore optimize the strategy of the venom.

APEKTx1 is the newest member of the type 2 sea anemone toxins directed towards voltage-gated potassium channels. To date, this family exists of only 4 other toxins, 3 kalicludines and SHTX II. Although it is known that these toxins are effective on  $K_v$  channels, little is known about their subtype selectivity. Here we report for the first time a screening of a type 2 toxin on a wide range of 23 different ion channels. This broad screening not only reveals a potent activity against  $K_v1.1$  ( $IC_{50} = 0.9 \pm 0.1$  nM) but also points out an impressive selectivity for these channels over the other isoforms tested. Even at concentrations 1000-fold higher than the  $IC_{50}$  value for  $K_v1.1$  channels, APEKTx1 has the ability to selectively inhibit this isoform subtype over others within the  $K_v1$  family. Moreover, A352P, E353S and Y379H substitutions in the  $K_v1.1$  subunit made these channels insensitive for APEKTx1 indicating that these 3 residues are critical for the toxin-channel interaction. Further electrophysiological characterization showed that this toxin does not modulate the voltage dependence of gating of  $K_v$  channels. The IV relationship in HK solution showed that ion selectivity was not changed after toxin binding. The observation that there is no difference in the percentage induced block either in ND96 or HK leads to the



1  
2  
3  
4 conclusion that channel blockage is independent of the direction of the potassium current flux and is not  
5 influenced by the extracellular concentration of  $K^+$  ions. Moreover, APEKTx1 did not show voltage  
6 dependence in its blockage of channels in a wide voltage range. The site of toxin binding is presumably  
7 located at the extracellular side since the inhibition of current through  $K_v1.1$  channels occurred rapidly  
8 and binding was reversible upon washout. We have shown that APEKTx1 shares not only sequence and  
9 structure homology with dendrotoxins (fig. 7) but also a similar activity profile with a comparable  
10 potency as these snake toxins. The APEKTx1 blockage followed the kinetic behavior of a bimolecular  
11 reaction as previously described for  $\alpha$ -DTX. The dendrotoxins have been extensively studied. The X-ray  
12 structure of  $\alpha$ -DTX and the NMR structure of DTX K have been reported [28,29]. They both possess  
13 structures which resemble very well the Kunitz-type serine protease inhibitors such as BPTI. The  
14 dendrotoxins have an N-terminal  $3_{10}$ -helix, a  $\beta$  hairpin and a C-terminal  $\alpha$ -helix. The residues important  
15 for their potent  $K_v$  blocking activity have been characterized. For DTX K, site-directed mutagenesis  
16 studies have shown that Lys3, Tyr4, Lys6, Pro8, Arg10, Trp25, Lys26 and Lys28 are the main residues  
17 involved in the interaction with the  $K_v1.1$  channels [30-32]. Among these, the basic residues in the  $3_{10}$ -  
18 helix, Lys3 and Lys6, have been pointed out as the key residues for toxin binding since mutation to an  
19 alanine led to a dramatic decrease in the ability to inhibit the  $K^+$  current [33]. Mutating the Pro8 and  
20 the Arg10 caused a 50- and 140-fold increase in  $IC_{50}$  value, respectively. The dramatic loss of affinity  
21 observed for DTX K binding to synaptic membranes when Trp25 and Lys26 were mutated to an alanine  
22 underlines that these residues are critical in recognition of  $K_v1.1$  channels [33,34]. Among these key  
23 residues, Pro8, Arg10 and Arg28 are conserved in APEKTx1.

24 For  $\alpha$ -DTX a mutational approach based on site-directed mutagenesis and chemical synthesis in which 31  
25 out of 59 amino acids were mutated, revealed that Arg1, Arg2, Lys3, Leu4, Ile6, Leu7 were crucial for  
26 channel blockage activity of this toxin. Substituting Arg1 by alanine resulted in a less than 10-fold  
27 decreased affinity, whereas Arg2, Leu4 and Ile6 substitution lowered the affinity 10 to 30 times. The  
28 Lys3 and Leu6 seem to be the most critical residues since mutating these amino acids resulted in a  
29 thousand times less potent toxins [30,31,35,36]. Of these residues critical for  $\alpha$ -DTX binding, the leu4  
30 and Ile6 are replaced by a homologous residue in APEKTx1.

31 These Lys3 and Leu6 residues in  $\alpha$ -DTX form the so-called dyad. It has been proposed that most toxins  
32 that block  $K_v$  channels possess a conserved functional core composed of a key basic residue (Lys or Arg)  
33 associated with a  $6.6 \pm 1$  Å distant key hydrophobic residue (Leu, Tyr or Phe). Such a functional dyad can  
34 be found in a broad range of structurally unrelated peptides from various animals such as scorpions, cone  
35 snails, snakes and sea anemones [37,38]. However, it has been reported that besides this dyad, other toxin  
36 determinants are required for a high affinity interaction between the toxin and his target [39]. Known  
37 examples of toxins lacking a dyad but still capable of blocking the  $K_v$  channel (or the other way around  
38 toxins with a dyad but incapable of blocking) strongly suggest that the functional dyad on its own cannot  
39 represent the minimal pharmacophore or prerequisite for  $K_v1$  binding [40,41]. Docking experiments with  
40 the scorpion toxin Pi1 and its homologs have highlighted that a ring of basic residues interacts with acidic  
41 residues of the  $K^+$  channel turret located in the most extracellular part of the channel outer vestibule. Pi1  
42 analogs, in which the basic residues from the ring were replaced by alanines, show a 50-480-fold  
43 reduction in peptide affinity for their target but were still able to block the potassium current [38]. In  
44 general, it is assumed that toxins recognize the  $K_v1$  subtypes through the interaction of various toxin  
45 residues, among which the basic ring, with certain residues of the  $K_v1$  channel turret. These interactions  
46 can be sufficient to inhibit the potassium current. Moreover, these specific molecular contacts determine  
47 toxin selectivity towards particular  $K_v1$  channel isoforms. The functional dyad can then be viewed as a  
48 secondary anchoring point, providing a higher toxin affinity without altering toxin selectivity. The side  
49 chain of the basic key residue enters the ion channel pore and is surrounded by four Asp residues of the P-  
50 loop selectivity filter. This Asp residue is highly conserved among all the  $K_v1$  channel isoforms. The  
51 carbonyl oxygen atoms of these Asp residues will form a stabilizing interaction with the side chain of the  
52 basic residue of the dyad. The key hydrophobic residue of the dyad will interact through both  
53 hydrophobic forces and hydrogen bonding with a cluster of aromatic residues in the P-loop. The specific  
54 positioning of the 2 residues from the dyad results in a physical barrier, especially because of the  
55  
56  
57  
58  
59  
60  
61  
62  
63  
64  
65

1  
2  
3  
4 positively charged side chain which is opposed to the  $K^+$  flux [42,43]. Because of the low identity with  
5 other  $K_V$  channel toxins and because none of the key residues critical for the  $K_V$  blockage of DTX K or  $\alpha$ -  
6 DTX are conserved in APEKTx1, we tried to hypothesize the key residues of APEKTx1 with the help of  
7 structural models. As it can be seen from figure 7, the role of a possible dyad in APEKTx1 can be  
8 fulfilled by Arg15 and Phe13, a basic and hydrophobic residues which are 6.2 Å separated. Assumably,  
9 the side chain of Arg15 enters the  $K_V1.1$  channel pore and interacts with the carbonyl oxygen atoms of the  
10 Asp377 residues. The Phe13 will most likely interact through hydrophobic forces with the aromatic  
11 cluster formed by Phe356, Trp364, Trp365, and Tyr375. Previous work has highlighted Tyr375 in  $K_V1.1$   
12 as a crucial residue for the selectivity of scorpion and sea anemone toxins [44]. The amino acid at this  
13 position is highly variable between  $K_V1$  isoforms and the nature of the side chain of this residue  
14 contributes significantly to the subtype selectivity of toxins. The observed 12000-fold decrease in affinity  
15 of APEKTx1 for mutated  $K_V1.1$  channels can be explained partially by the Y379H mutation. The same  
16 mutation prevented the  $K_V1.1$  binding of another sea anemone toxin BgK, which binds to wild type  
17 channels with an  $IC_{50}$  value of 0.7 nM [43-46]. The E353 also seems to be critical for interaction with  
18 APEKTx1. *Hurst et al* have shown that each of the 3 mutations on its own decreased dendrotoxin potency  
19 and that the removal of a negative charge at position 353 caused the greatest decrease in affinity [24].  
20 However, simultaneous substitution of all 3 residues caused a much stronger decrease in DTX sensitivity  
21 than the single mutations. Further site-directed mutagenesis studies or ideally co-crystallization studies  
22 are required to elucidate if such subtle changes in sequence of the pore region are responsible for the  
23 dramatically loss of sensitivity of  $K_V1.1$  for this toxin.

24 Also shown in figure 7 are the basic residues which are conserved in DTX K and  $\alpha$ -DTX. These residues  
25 possibly contribute to the basic ring important for recognition, interaction and correct positioning of the  
26 toxin on the channel. As mentioned above, previous work has shown that mutating these conserved  
27 residues leads to affinity loss in DTX K or  $\alpha$ -DTX [30]. However, this is only a hypothesis which requires  
28 further conformation from site-directed mutagenesis studies, docking experiments and structure analysis.

29 The bovine pancreatic trypsin inhibitor belongs to the Kunitz-type inhibitors and is a potent inhibitor of  
30 serine proteases. The crystal structures of BPTI with bovine trypsin and with bovine chymotrypsin have  
31 been determined [47-49]. Analysis of these complexes have shown that there are 10-13 residues on the  
32 inhibitor forming less than 4 Å contacts with 20-25 residues of the enzyme. The 13 key residues of the  
33 inhibitor form a structural epitope seen as two extended and exposed loops. The first loop which is the  
34 primary contact site is composed of the residues Thr11 to Ile19. The second loop is more C-terminal  
35 situated and is formed by residues Gly36 to Arg39 [50,51]. The Lys15 has been pinpointed as a single  
36 residue hot spot responsible for a major part of the enzyme-inhibitor contacts. The side chain of this basic  
37 amino acid penetrates deeply into the specificity binding pocket of the protease where it electrostatically  
38 interacts with the Asp189 of the protease. This Lys15-Asp189 interaction delivers the major contribution  
39 to the association energy for the BPTI-trypsin complex. The role of Lys15 as a crucial player in the  
40 energetics of the recognition was demonstrated by substituting this residue with Gly. The point mutation  
41 reduced the total association energy with 70% leading to an association constant decreased by 9 orders of  
42 magnitude. Structure determination of  $\alpha$ -DTX provided an explanation why this toxin and its homologue  
43 DTX I cannot inhibit proteases. The basic amino acid in BPTI has been replaced in  $\alpha$ -DTX by a Tyr  
44 incapable of interacting effectively with binding pocket of trypsin [52-54]. Further explanation for the  
45 lack of protease inhibition by the dendrotoxins can be found in the presence of Asp17 in  $\alpha$ -DTX, Glu17 in  
46 DTX I and Arg16 in DTX K. The existence of these longer amino acid residues in dendrotoxins instead of  
47 the smaller alanine in BPTI causes a most unfavorable complex with the trypsin binding site. Moreover,  
48 the Pro19 in DTX K and Pro21 in DTX I and  $\alpha$ -DTX instead of the Ile19 in BPTI greatly impedes a good  
49 interaction with the side chain of the Tyr39 of trypsin. The residues essential for kunitz-type inhibition in  
50 the primary contact site (Gly12, Cys14, Lys15 and Ala16) are all conserved in APEKTx1 except for the  
51 Arg15 (fig. 7). However, previous residue-specific modification studies have shown that mutating the Lys  
52 15 to Arg did not alter the association constant. The lower protease inhibition activity of APEKTx1  
53 compared to BPTI (fig.5) can be explained by the presence of Phe13 and Pro19. A double BPTI mutant  
54 with a phenylalanine at position 13 and an arginine at position 15, exactly as in APEKTx1, resulted in a  
55  
56  
57  
58  
59  
60  
61  
62  
63  
64  
65

1  
2  
3  
4 100-fold decreased association constant compared to the wild type [54]. The unfavorable interaction of  
5 Pro19 with trypsin has been described above.  
6

## 7 5. Conclusion

8  
9 We have demonstrated the unique dual function of APEKTx1, which is a competitive Kunitz-type  
10 protease inhibitor and a very potent and selective  $K_V1.1$  channel blocker. Moreover, several amino acid  
11 residues have been suggested to play a functionally critical role in the high potency and unique selectivity  
12 of this toxin. Further structure-function analysis involving site-directed mutagenesis studies, docking  
13 experiments and NMR are required in order to confirm their role. Because of its high affinity and  
14 selectivity, APEKTx1 might be a very interesting probe for further characterization of the binding sites of  
15  $K_V1.1$  channels. Finally, APEKTx1 represents a valuable tool to examine the exact role of  $K_V1.1$  in  
16 various channelopathies, and might serve as a lead compound in the development of novel therapeutical  
17 agents for these diseases.  
18  
19  
20  
21

22 **Acknowledgments** We would like to thank O. Pongs for sharing the r $K_V1.2$ , r $K_V1.4$ , and rKV1.5 and  
23 r $K_V1.6$  cDNA. We are grateful to M.L. Garcia for sharing the h $K_V1.3$  clone and to DJ Snyders for sharing  
24 the r $K_V2.1$ , h $K_V3.1$ , rKV4.2 and r $K_V4.3$ . The Shaker IR clone was kindly provided by G. Yellen. We  
25 thank M. Keating for sharing hERG, John N. Wood for sharing r $Na_V1.8$ , A.L. Goldin for sharing r $Na_V1.2$ ,  
26 r $Na_V1.3$  and m $Na_V1.6$ , G. Mandel for sharing r $Na_V1.4$ , R.G. Kallen for sharing h $Na_V1.5$ , S.H. Heinemann  
27 for sharing the rat $\beta 1$  subunit, S.C. Cannon for sharing the h $\beta 1$  subunit and Martin S. Williamson for  
28 providing the Para and tipE clone. The  $Na_V1.7$  clone was kindly provided by Roche. The authors would  
29 like to thank Prof. Dr. Dr.h.c. Wolf-Georg Forssmann, Dr. Eva Cuypers for the useful discussions, Dr.  
30 Elia Diego-García for helpful suggestions and Annelies Van Der Haegen for help with the modeling. This  
31 work was supported by the following grants: G.0257.08 and G.0330.06 (F.W.O. Vlaanderen), OT-05-64  
32 (K.U. Leuven), UA P6/31 (IAP), P6/28 (IAP), GOA 08/16 (K.U.Leuven).  
33  
34

35 **Conflict of interest** The authors declare that they have no conflict of interest.  
36

## 37 Reference

- 38  
39  
40 [1] Gutman, G.A., Chandy, K.G., Grissmer, S., Lazdunski, M., McKinnon, D., Pardo, L.A.,  
41 Robertson, G.A., Rudy, B., Sanguinetti, M.C., Stuhmer, W. and Wang, X., International Union of  
42 Pharmacology. LIII. Nomenclature and molecular relationships of voltage-gated potassium  
43 channels, *Pharmacol Rev* 57 (2005) 473-508.  
44 [2] Lujan, R., Organisation of potassium channels on the neuronal surface, *J Chem Neuroanat* 40  
45 (2010) 1-20.  
46 [3] Yu, F.H., Yarov-Yarovoy, V., Gutman, G.A. and Catterall, W.A., Overview of molecular  
47 relationships in the voltage-gated ion channel superfamily, *Pharmacol Rev* 57 (2005) 387-395.  
48 [4] Pongs, O., Voltage-gated potassium channels: from hyperexcitability to excitement, *FEBS Lett*  
49 452 (1999) 31-35.  
50 [5] Bezanilla, F., The voltage sensor in voltage-dependent ion channels, *Physiol Rev* 80 (2000) 555-  
51 592.  
52 [6] Swartz, K.J., Towards a structural view of gating in potassium channels, *Nat Rev Neurosci* 5  
53 (2004) 905-916.  
54 [7] Jiang, B., Sun, X., Cao, K. and Wang, R., Endogenous Kv channels in human embryonic kidney  
55 (HEK-293) cells, *Mol Cell Biochem* 238 (2002) 69-79.  
56 [8] Oquadid-Ahidouch, H., Chaussade, F., Roudbaraki, M., Slomianny, C., Dewailly, E., Delcourt, P.  
57 and Prevarskaya, N., KV1.1 K(+) channels identification in human breast carcinoma cells:  
58 involvement in cell proliferation, *Biochem Biophys Res Commun* 278 (2000) 272-277.  
59  
60  
61  
62  
63  
64  
65

- 1  
2  
3  
4 [9] Andreev, Y.A., Kozlov, S.A., Koshelev, S.G., Ivanova, E.A., Monastyrnaya, M.M., Kozlovskaya,  
5 E.P. and Grishin, E.V., Analgesic compound from sea anemone *Heteractis crispa* is the first  
6 polypeptide inhibitor of vanilloid receptor 1 (TRPV1), *J Biol Chem* 283 (2008) 23914-23921.  
7 [10] Honma, T. and Shiomi, K., Peptide toxins in sea anemones: structural and functional aspects, *Mar*  
8 *Biotechnol* (NY) 8 (2006) 1-10.  
9 [11] Castaneda, O. and Harvey, A.L., Discovery and characterization of cnidarian peptide toxins that  
10 affect neuronal potassium ion channels, *Toxicon* 54 (2009) 1119-1124.  
11 [12] Bosmans, F. and Tytgat, J., Sea anemone venom as a source of insecticidal peptides acting on  
12 voltage-gated Na<sup>+</sup> channels, *Toxicon* 49 (2007) 550-560.  
13 [13] Oliveira, J.S., Zaharenko, A.J., Ferreira, W.A., Jr., Konno, K., Shida, C.S., Richardson, M.,  
14 Lucio, A.D., Beirao, P.S. and de Freitas, J.C., BcIV, a new paralyzing peptide obtained from the  
15 venom of the sea anemone *Bunodosoma caissarum*. A comparison with the Na<sup>+</sup> channel toxin  
16 BcIII, *Biochim Biophys Acta* 1764 (2006) 1592-1600.  
17 [14] Diochot, S. and Lazdunski, M., Sea anemone toxins affecting potassium channels, *Prog Mol*  
18 *Subcell Biol* 46 (2009) 99-122.  
19 [15] Diochot, S., Baron, A., Rash, L.D., Deval, E., Escoubas, P., Scarzello, S., Salinas, M. and  
20 Lazdunski, M., A new sea anemone peptide, APETx2, inhibits ASIC3, a major acid-sensitive  
21 channel in sensory neurons, *Embo J* 23 (2004) 1516-1525.  
22 [16] Bruhn, T., Schaller, C., Schulze, C., Sanchez-Rodriguez, J., Dannmeier, C., Ravens, U., Heubach,  
23 J.F., Eckhardt, K., Schmidtmayer, J., Schmidt, H., Aneiros, A., Wachter, E. and Beress, L.,  
24 Isolation and characterisation of five neurotoxic and cardiotoxic polypeptides from the sea  
25 anemone *Anthopleura elegantissima*, *Toxicon* 39 (2001) 693-702.  
26 [17] Diochot, S., Loret, E., Bruhn, T., Beress, L. and Lazdunski, M., APETx1, a new toxin from the  
27 sea anemone *Anthopleura elegantissima*, blocks voltage-gated human ether-a-go-go-related gene  
28 potassium channels, *Mol Pharmacol* 64 (2003) 59-69.  
29 [18] Salceda, E., Garateix, A., Aneiros, A., Salazar, H., Lopez, O. and Soto, E., Effects of ApC, a sea  
30 anemone toxin, on sodium currents of mammalian neurons, *Brain Res* 1110 (2006) 136-143.  
31 [19] Schaller, H.C. and Bodenmuller, H., Isolation and amino acid sequence of a morphogenetic  
32 peptide from hydra, *Proc Natl Acad Sci U S A* 78 (1981) 7000-7004.  
33 [20] Liman, E.R., Tytgat, J. and Hess, P., Subunit stoichiometry of a mammalian K<sup>+</sup> channel  
34 determined by construction of multimeric cDNAs, *Neuron* 9 (1992) 861-871.  
35 [21] Schweitz, H., Bruhn, T., Guillemare, E., Moinier, D., Lancelin, J.M., Beress, L. and Lazdunski,  
36 M., Kalicludines and kaliseptine. Two different classes of sea anemone toxins for voltage  
37 sensitive K<sup>+</sup> channels, *J Biol Chem* 270 (1995) 25121-25126.  
38 [22] Honma, T., Kawahata, S., Ishida, M., Nagai, H., Nagashima, Y. and Shiomi, K., Novel peptide  
39 toxins from the sea anemone *Stichodactyla haddoni*, *Peptides* 29 (2008) 536-544.  
40 [23] Tytgat, J., Debont, T., Carmeliet, E. and Daenens, P., The alpha-dendrotoxin footprint on a  
41 mammalian potassium channel, *J Biol Chem* 270 (1995) 24776-24781.  
42 [24] Hurst, R.S., Busch, A.E., Kavanaugh, M.P., Osborne, P.B., North, R.A. and Adelman, J.P.,  
43 Identification of amino acid residues involved in dendrotoxin block of rat voltage-dependent  
44 potassium channels, *Mol Pharmacol* 40 (1991) 572-576.  
45 [25] MacKinnon, R. and Miller, C., Mutant potassium channels with altered binding of charybdotoxin,  
46 a pore-blocking peptide inhibitor, *Science* 245 (1989) 1382-1385.  
47 [26] Akhtar, S., Shamotienko, O., Papakosta, M., Ali, F. and Dolly, J.O., Characteristics of brain Kv1  
48 channels tailored to mimic native counterparts by tandem linkage of alpha subunits: implications  
49 for K<sup>+</sup> channelopathies, *J Biol Chem* 277 (2002) 16376-16382.  
50 [27] Robertson, B., Owen, D., Stow, J., Butler, C. and Newland, C., Novel effects of dendrotoxin  
51 homologues on subtypes of mammalian Kv1 potassium channels expressed in *Xenopus* oocytes,  
52 *FEBS Lett* 383 (1996) 26-30.  
53  
54  
55  
56  
57  
58  
59  
60  
61  
62  
63  
64  
65

- 1  
2  
3  
4 [28] Skarzynski, T., Crystal structure of alpha-dendrotoxin from the green mamba venom and its  
5 comparison with the structure of bovine pancreatic trypsin inhibitor, *J Mol Biol* 224 (1992) 671-  
6 683.
- 7 [29] Berndt, K.D., Guntert, P. and Wuthrich, K., Nuclear magnetic resonance solution structure of  
8 dendrotoxin K from the venom of *Dendroaspis polylepis polylepis*, *J Mol Biol* 234 (1993) 735-  
9 750.
- 10 [30] Harvey, A.L. and Robertson, B., Dendrotoxins: structure-activity relationships and effects on  
11 potassium ion channels, *Curr Med Chem* 11 (2004) 3065-3072.
- 12 [31] Gasparini, S., Danse, J.M., Lecoq, A., Pinkasfeld, S., Zinn-Justin, S., Young, L.C., de Medeiros,  
13 C.C., Rowan, E.G., Harvey, A.L. and Menez, A., Delineation of the functional site of alpha-  
14 dendrotoxin. The functional topographies of dendrotoxins are different but share a conserved core  
15 with those of other Kv1 potassium channel-blocking toxins, *J Biol Chem* 273 (1998) 25393-  
16 25403.
- 17 [32] Imredy, J.P. and MacKinnon, R., Energetic and structural interactions between delta-dendrotoxin  
18 and a voltage-gated potassium channel, *J Mol Biol* 296 (2000) 1283-1294.
- 19 [33] Wang, F.C., Bell, N., Reid, P., Smith, L.A., McIntosh, P., Robertson, B. and Dolly, J.O.,  
20 Identification of residues in dendrotoxin K responsible for its discrimination between neuronal  
21 K<sup>+</sup> channels containing Kv1.1 and 1.2 alpha subunits, *Eur J Biochem* 263 (1999) 222-229.
- 22 [34] Smith, L.A., Reid, P.F., Wang, F.C., Parcej, D.N., Schmidt, J.J., Olson, M.A. and Dolly, J.O.,  
23 Site-directed mutagenesis of dendrotoxin K reveals amino acids critical for its interaction with  
24 neuronal K<sup>+</sup> channels, *Biochemistry* 36 (1997) 7690-7696.
- 25 [35] Danse, J.M., Rowan, E.G., Gasparini, S., Ducancel, F., Vatanpour, H., Young, L.C., Poorheidari,  
26 G., Lajeunesse, E., Drevet, P., Menez, R. and et al., On the site by which alpha-dendrotoxin binds  
27 to voltage-dependent potassium channels: site-directed mutagenesis reveals that the lysine triplet  
28 28-30 is not essential for binding, *FEBS Lett* 356 (1994) 153-158.
- 29 [36] Harvey, A.L., Recent studies on dendrotoxins and potassium ion channels, *Gen Pharmacol* 28  
30 (1997) 7-12.
- 31 [37] Dauplais, M., Lecoq, A., Song, J., Cotton, J., Jamin, N., Gilquin, B., Roumestand, C., Vita, C., de  
32 Medeiros, C.L., Rowan, E.G., Harvey, A.L. and Menez, A., On the convergent evolution of  
33 animal toxins. Conservation of a diad of functional residues in potassium channel-blocking toxins  
34 with unrelated structures, *J Biol Chem* 272 (1997) 4302-4309.
- 35 [38] Mouhat, S., Mosbah, A., Visan, V., Wulff, H., Delepierre, M., Darbon, H., Grissmer, S., De  
36 Waard, M. and Sabatier, J.M., The 'functional' dyad of scorpion toxin Pi1 is not itself a  
37 prerequisite for toxin binding to the voltage-gated Kv1.2 potassium channels, *Biochem J* 377  
38 (2004) 25-36.
- 39 [39] MacKinnon, R., Cohen, S.L., Kuo, A., Lee, A. and Chait, B.T., Structural conservation in  
40 prokaryotic and eukaryotic potassium channels, *Science* 280 (1998) 106-109.
- 41 [40] Shon, K.J., Stocker, M., Terlau, H., Stuhmer, W., Jacobsen, R., Walker, C., Grille, M., Watkins,  
42 M., Hillyard, D.R., Gray, W.R. and Olivera, B.M., kappa-Conotoxin PVIIA is a peptide inhibiting  
43 the shaker K<sup>+</sup> channel, *J Biol Chem* 273 (1998) 33-38.
- 44 [41] Huys, I., Xu, C.Q., Wang, C.Z., Vacher, H., Martin-Eauclaire, M.F., Chi, C.W. and Tytgat, J.,  
45 BmTx3, a scorpion toxin with two putative functional faces separately active on A-type K<sup>+</sup> and  
46 HERG currents, *Biochem J* 378 (2004) 745-752.
- 47 [42] Mouhat, S., De Waard, M. and Sabatier, J.M., Contribution of the functional dyad of animal  
48 toxins acting on voltage-gated Kv1-type channels, *J Pept Sci* 11 (2005) 65-68.
- 49 [43] Jouirou, B., Mouhat, S., Andreotti, N., De Waard, M. and Sabatier, J.M., Toxin determinants  
50 required for interaction with voltage-gated K<sup>+</sup> channels, *Toxicon* 43 (2004) 909-914.
- 51 [44] Gilquin, B., Braud, S., Eriksson, M.A., Roux, B., Bailey, T.D., Priest, B.T., Garcia, M.L., Menez,  
52 A. and Gasparini, S., A variable residue in the pore of Kv1 channels is critical for the high  
53 affinity of blockers from sea anemones and scorpions, *J Biol Chem* 280 (2005) 27093-27102.
- 54  
55  
56  
57  
58  
59  
60  
61  
62  
63  
64  
65

- 1  
2  
3  
4 [45] Visan, V., Fajloun, Z., Sabatier, J.M. and Grissmer, S., Mapping of maurotoxin binding sites on  
5 hKv1.2, hKv1.3, and hKCa1 channels, *Mol Pharmacol* 66 (2004) 1103-1112.  
6 [46] Alessandri-Haber, N., Lecoq, A., Gasparini, S., Grangier-Macmath, G., Jacquet, G., Harvey,  
7 A.L., de Medeiros, C., Rowan, E.G., Gola, M., Menez, A. and Crest, M., Mapping the functional  
8 anatomy of BgK on Kv1.1, Kv1.2, and Kv1.3. Clues to design analogs with enhanced selectivity,  
9 *J Biol Chem* 274 (1999) 35653-35661.  
10 [47] Helland, R., Otlewski, J., Sundheim, O., Dadlez, M. and Smalas, A.O., The crystal structures of  
11 the complexes between bovine beta-trypsin and ten P1 variants of BPTI, *J Mol Biol* 287 (1999)  
12 923-942.  
13 [48] Capasso, C., Rizzi, M., Menegatti, E., Ascenzi, P. and Bolognesi, M., Crystal structure of the  
14 bovine alpha-chymotrypsin:Kunitz inhibitor complex. An example of multiple protein:protein  
15 recognition sites, *J Mol Recognit* 10 (1997) 26-35.  
16 [49] Scheidig, A.J., Hynes, T.R., Pelletier, L.A., Wells, J.A. and Kossiakoff, A.A., Crystal structures  
17 of bovine chymotrypsin and trypsin complexed to the inhibitor domain of Alzheimer's amyloid  
18 beta-protein precursor (APPI) and basic pancreatic trypsin inhibitor (BPTI): engineering of  
19 inhibitors with altered specificities, *Protein Sci* 6 (1997) 1806-1824.  
20 [50] Krowarsch, D., Dadlez, M., Buczek, O., Krokoszynska, I., Smalas, A.O. and Otlewski, J.,  
21 Interscaffolding additivity: binding of P1 variants of bovine pancreatic trypsin inhibitor to four  
22 serine proteases, *J Mol Biol* 289 (1999) 175-186.  
23 [51] Buczek, O., Koscielska-Kasprzak, K., Krowarsch, D., Dadlez, M. and Otlewski, J., Analysis of  
24 serine proteinase-inhibitor interaction by alanine shaving, *Protein Sci* 11 (2002) 806-819.  
25 [52] Czapinska, H. and Otlewski, J., Structural and energetic determinants of the S1-site specificity in  
26 serine proteases, *Eur J Biochem* 260 (1999) 571-595.  
27 [53] Lancelin, J.M., Foray, M.F., Poncin, M., Hollecker, M. and Marion, D., Proteinase inhibitor  
28 homologues as potassium channel blockers, *Nat Struct Biol* 1 (1994) 246-250.  
29 [54] Krowarsch, D. and Otlewski, J., Amino-acid substitutions at the fully exposed P1 site of bovine  
30 pancreatic trypsin inhibitor affect its stability, *Protein Sci* 10 (2001) 715-724.  
31  
32  
33  
34  
35  
36

### Footnotes

37  
38  
39 § To whom correspondence should be addressed. Tel.: +32 1632 34 03; Fax: +32 16 32 34 05; E-mail:  
40 [jan.tytgat@pharm.kuleuven.be](mailto:jan.tytgat@pharm.kuleuven.be)

41 The abbreviations used are: APEKTx1, Anthopleura elegantissima potassium channel toxin 1; MALDI  
42 TOF, matrix-assisted laser desorption-ionization time of flight; RP-HPLC, reversed-phase high  
43 performance liquid chromatography; TFA, trifluoroacetic acid; K<sub>v</sub> channel, voltage-gated potassium  
44 channel; DTX; dendrotoxin; BPTI, bovine pancreatic trypsin inhibitor.  
45  
46

### Figure Legends

#### Fig. 1: Purification of APEKTx1.

47  
48  
49 A, the crude fraction found to be active in the electrophysiological screening was loaded on a C18 column  
50 with a linear gradient of 0.085% TFA in acetonitrile. Only the fraction containing the largest peak  
51 indicated by the arrow was active on K<sub>v</sub>1.1 channels. B, this active fraction was further purified using the  
52 same conditions as in A.  
53

#### Fig. 2: Alignment.

54  
55 Amino acid sequence of APEKTx1 and alignment with the other members of the type 2 sea anemone  
56 toxins, dendrotoxins, protease inhibitors from sea anemones and BPTI. Amino acid residues identical  
57 with APEKTx1 are shown on grey background, cysteine residues are printed in red. Disulfide bridge  
58 pattern based on AsKC3 are indicated. AsKC1-3 from *Anemonia sulcata*, AFAPI-I and AFAPI-III from  
59 *Anthopleura fuscoviridis*, AXPI-II from *Anthopleura xanthogrammica*, DTX E from *Dendroaspis*  
60  
61  
62  
63  
64  
65

1  
2  
3  
4 *polylepis polylepis*, SHTX III from *Stichodactyla haddoni*, DTX K from *Dendroaspis polylepis*,  $\alpha$ -DTX  
5 from and BPTI from *Bos taurus*.

6 **Fig. 3: Activity of APEKTx1 on K<sub>V</sub> channels.**

7 **A**, Differential effects of APEKTx1 on several cloned voltage gated potassium and sodium channel  
8 isoforms expressed in *X. laevis* oocytes. Representative whole-cell current traces in control and toxin  
9 conditions are shown. The dotted line indicates the zero-current level. The asterisk (\*) marks steady-state  
10 current traces after application of 1  $\mu$ M of APEKTx1. This screening on a large number of K<sub>V</sub> channel  
11 isoforms belonging to different subfamilies of the voltage gated potassium channel family shows that  
12 APEKTx1 selectively blocks K<sub>V</sub>1.1 channels at a concentration of 1  $\mu$ M. Traces shown are representative  
13 traces of at least 3 independent experiments ( $n \geq 3$ ).

14 **B**, Original traces for wild type K<sub>V</sub>1.1 channels with application of 0.3, 1 and 3 nM APEKTx1. For  
15 mutant K<sub>V</sub>1.1 channels original traces with application of 100  $\mu$ M APEKTx1 are also shown.

16 **Fig. 4: Effects on K<sub>V</sub>1.1 channel gating.**

17 **A**, dose-response curve on wild-type (closed symbols) and triple mutant (open symbols) K<sub>V</sub>1.1 channels  
18 obtained by plotting the percentage blocked current as a function of increasing toxin concentrations. For  
19 APEKTx1 (triangles), IC<sub>50</sub> values yielded  $0.9 \pm 0.1$  nM and  $10.8 \pm 0.6$   $\mu$ M for wild type and mutant  
20 channels, respectively. For DTX K (squares), IC<sub>50</sub> values were determined at  $0.51 \pm 0.064$  nM and  $5.28 \pm$   
21  $0.2$  nM for wild-type and mutant channels, respectively.

22 **B**, the percentage of residual current after application of 10 nM APEKTx1 as a function of membrane  
23 potential. In a range of test potentials from -30 mV to +40 mV, no difference in the degree of APEKTx1  
24 induced block could be observed.

25 **C and D**, show *IV* and *gV* curves in ND96 and HK respectively. APEKTx1 does not act as a gating  
26 modifier. In ND96, the  $V_{1/2}$  in control (open circles) and in the presence of 10 nM APEKTx1 (closed  
27 circles) was characterized by a value of  $-15.7 \pm 1.23$  mV ( $n=5$ ) and  $-12.71 \pm 0.5$  mV ( $n=6$ ) respectively. In  
28 HK, the  $V_{1/2}$  yielded respectively,  $-25.84 \pm 2.53$  mV and  $-19.89 \pm 3.2$  mV. No significant shift was  
29 observed. Moreover, APEKTx1 did not significantly alter the reversal potential.

30 **E**, fast kinetics of inhibition of K<sub>V</sub>1.1 channels and reversibility of the inhibition upon washout. Control  
31 (open triangles), wash-in, (open triangles+ black bar), wash-out (open circles). Values for  $\tau_{on}$  and  $\tau_{off}$  in  
32 this experiment were 92.7 and 47s, respectively.

33 **F**, APEKTx1 blockage followed the kinetic behavior of a bimolecular reaction as proposed by Tytgat *et*  
34 *al.* Displayed are the effects of increasing concentrations APEKTx1 on a K<sub>V</sub>1.1 channel. The apparent  
35 first order association rate constant  $k_{on}$  (open circles) increased linearly with the toxin concentration. The  
36 second order dissociation constant  $k_{off}$  (closed circles) remained constant. Both these values are in  
37 correlation with the scheme of a bimolecular reaction.

38 **Fig. 5: Alignment of the pore regions of K<sub>V</sub>1 family.**

39 Sequence alignment of the pore region of K<sub>V</sub>1.1-K<sub>V</sub>1.6 and the K<sub>V</sub>1.1 mutant. The 3 mutated residues  
40 (A352P, E353S and Y379H) in the K<sub>V</sub>1.1 mutant are shown in red. Asp377, important for stabilizing the  
41 side chain of the basic residue of the dyad is shown in blue while the residue from the aromatic cluster  
42 (Phe356, Trp364, Trp365, Tyr375) which interacts with the hydrophobic residue of the dyad are shown in  
43 green.

44 **Fig. 6: Kunitz-type protease inhibition.**

45 The figure shows the concentration dependence of trypsin inhibition by different concentrations of BPTI,  
46 closed circles; APEKTx1, open circles; DTX I, open triangles and DTX K, open squares. A 3-fold  
47 molecular excess of APEKTx1 over trypsin inhibited the paranitroaniline release completely

48 **Fig. 7: Spatial structure models of  $\alpha$ -DTX, DTX K, BPTI and APEKTx1.**

49 Structural models for  $\alpha$ -DTX (PDB accession code 1DTX), DTX K (1DTK), BPTI (1PIT) and APEKTx1.  
50 The model of APEKTx1 was built on the basis of the structure of the homologue snake protease inhibitor  
51 textilinin (3BYB). Residues known to be important for K<sub>V</sub> channel blockade ( $\alpha$ -DTX, DTX K,  
52 APEKTx1) are indicated in red. The model for APEKTx1 shows the residues possibly forming a dyad in  
53 red, the residues possibly contributing to the basic ring are shown in green. The residues known to be  
54  
55  
56  
57  
58  
59  
60  
61  
62  
63  
64  
65

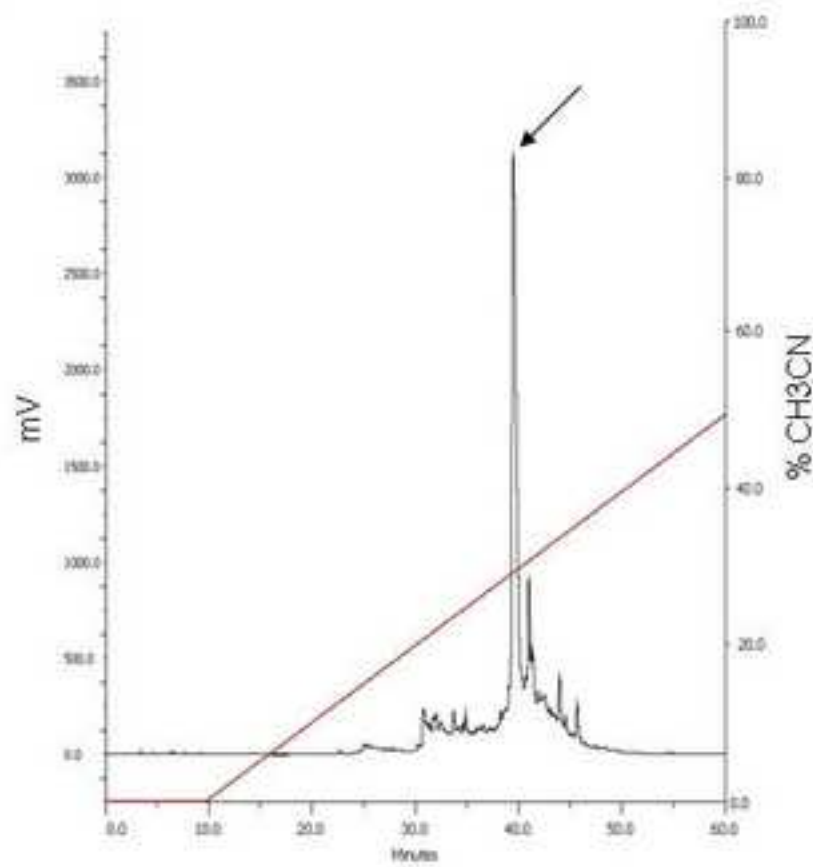
1  
2  
3  
4 important for protease inhibition (BPTI and APEKTx1) are colored in blue (primary contact site) and in  
5 yellow (secondary contact site).  
6  
7  
8  
9  
10  
11  
12  
13  
14  
15  
16  
17  
18  
19  
20  
21  
22  
23  
24  
25  
26  
27  
28  
29  
30  
31  
32  
33  
34  
35  
36  
37  
38  
39  
40  
41  
42  
43  
44  
45  
46  
47  
48  
49  
50  
51  
52  
53  
54  
55  
56  
57  
58  
59  
60  
61  
62  
63  
64  
65

Accepted Manuscript



Figure 1

A



B

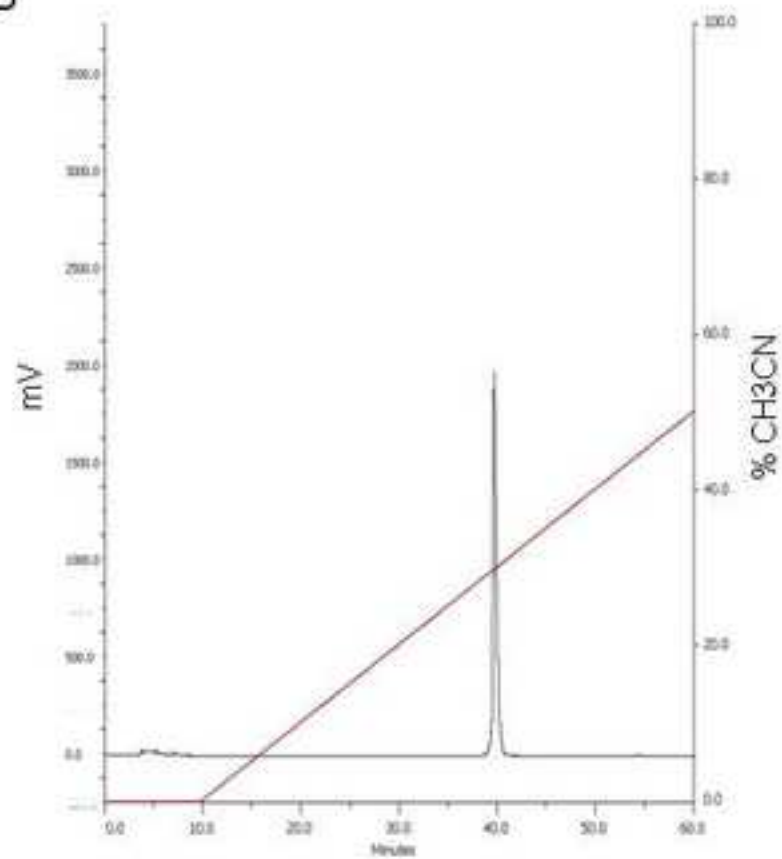


Figure 2

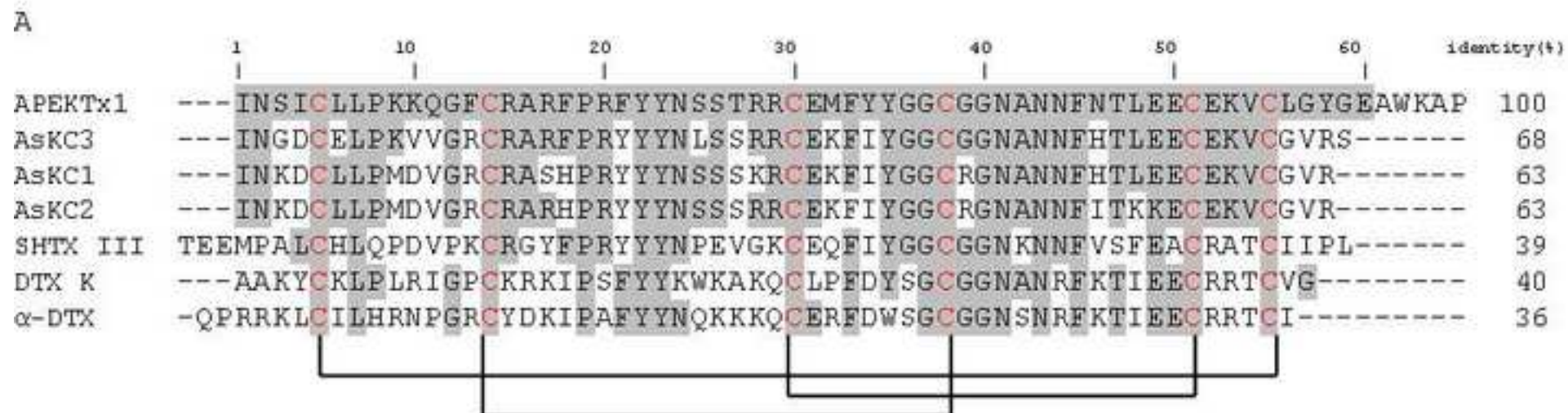
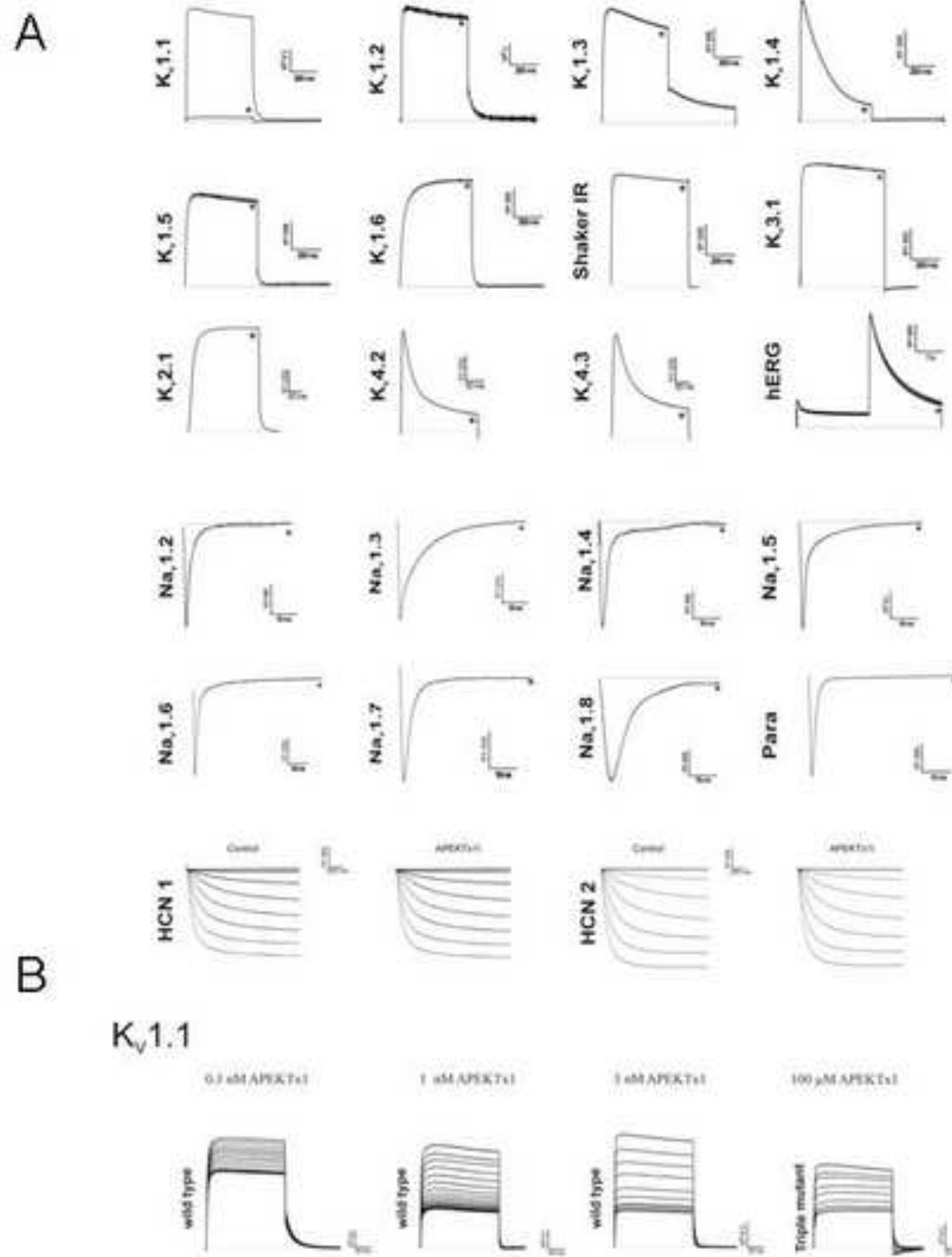
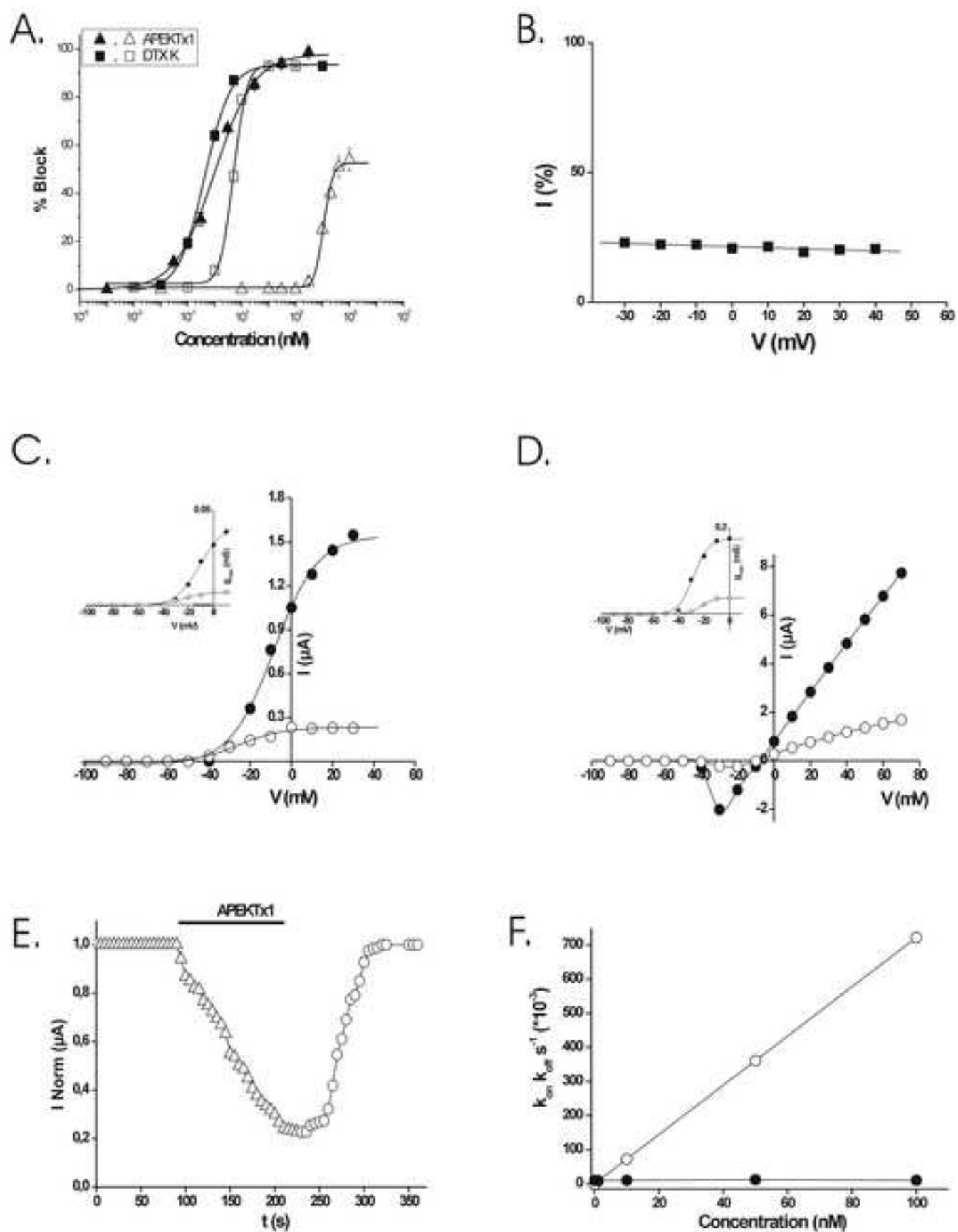


Figure 3





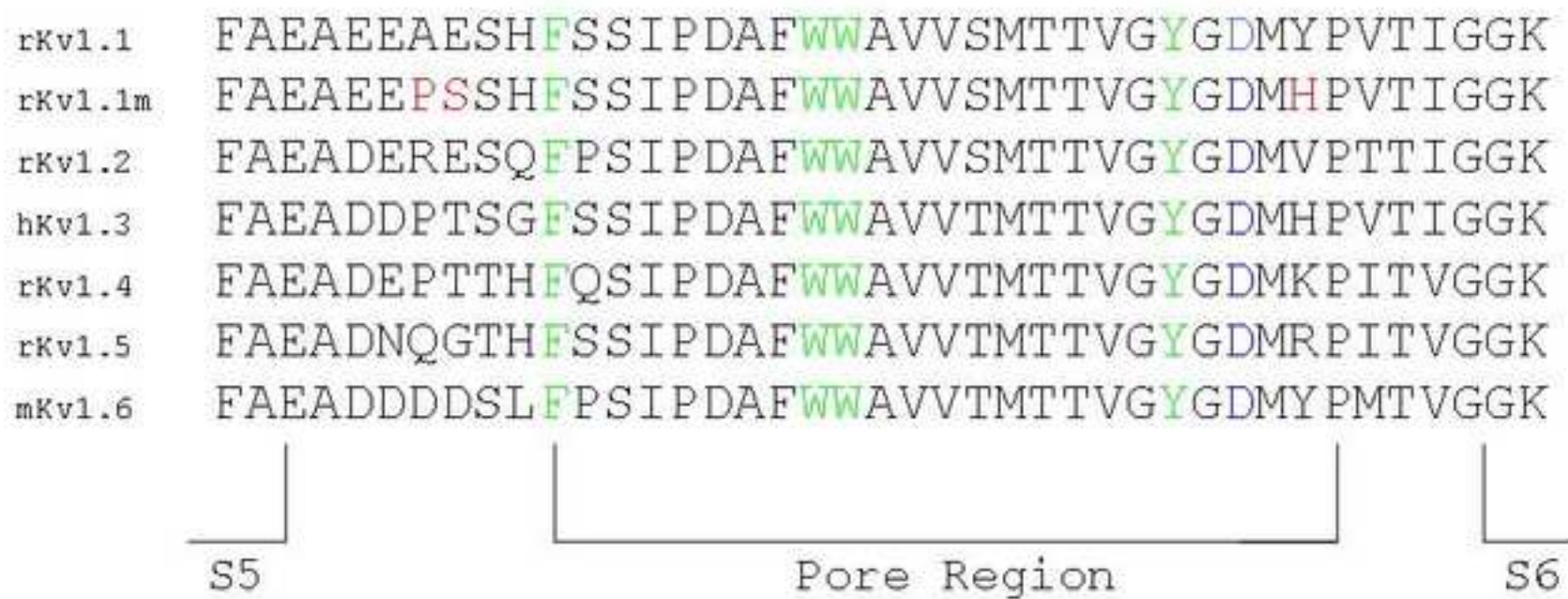


Figure 6

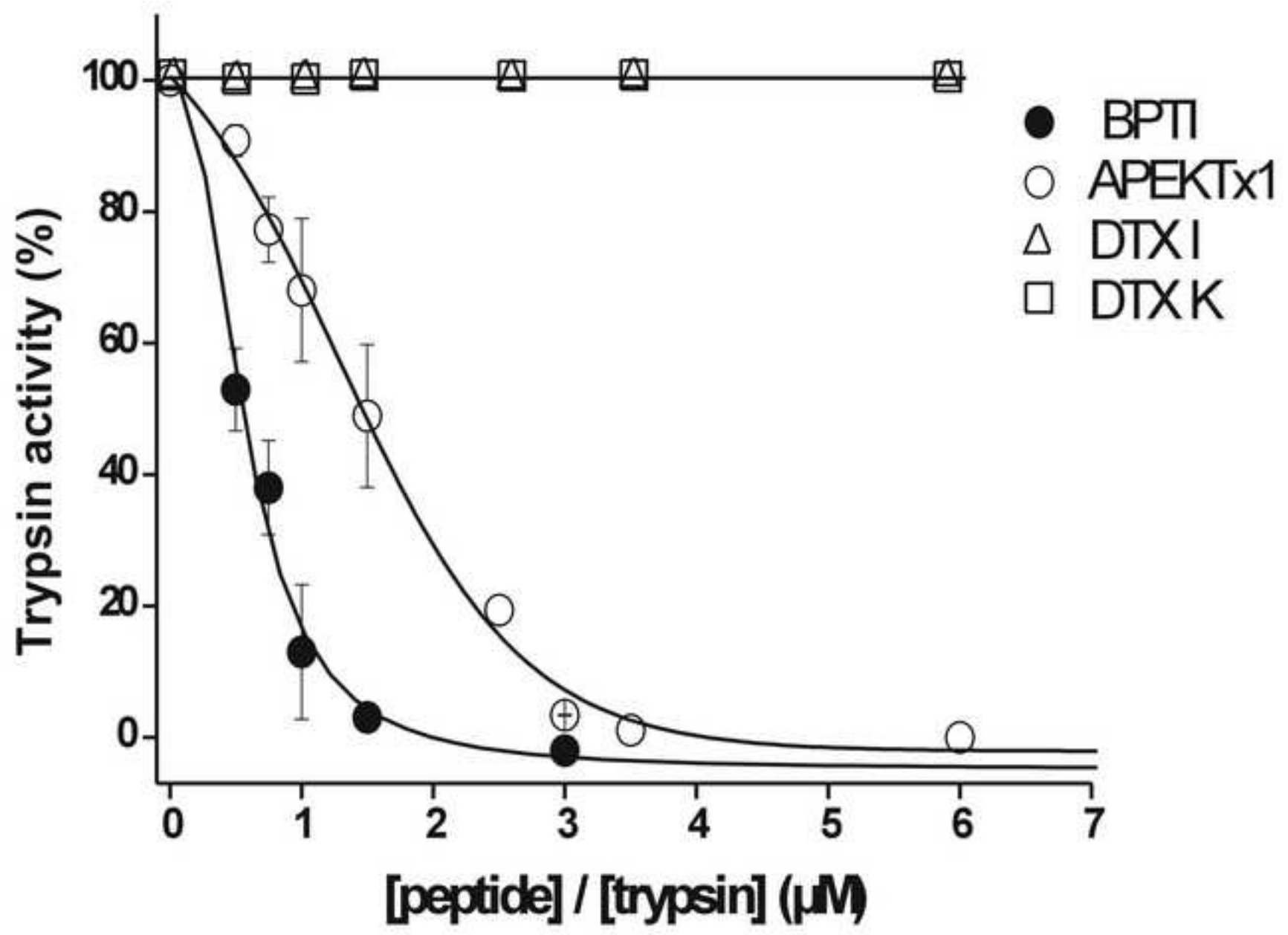
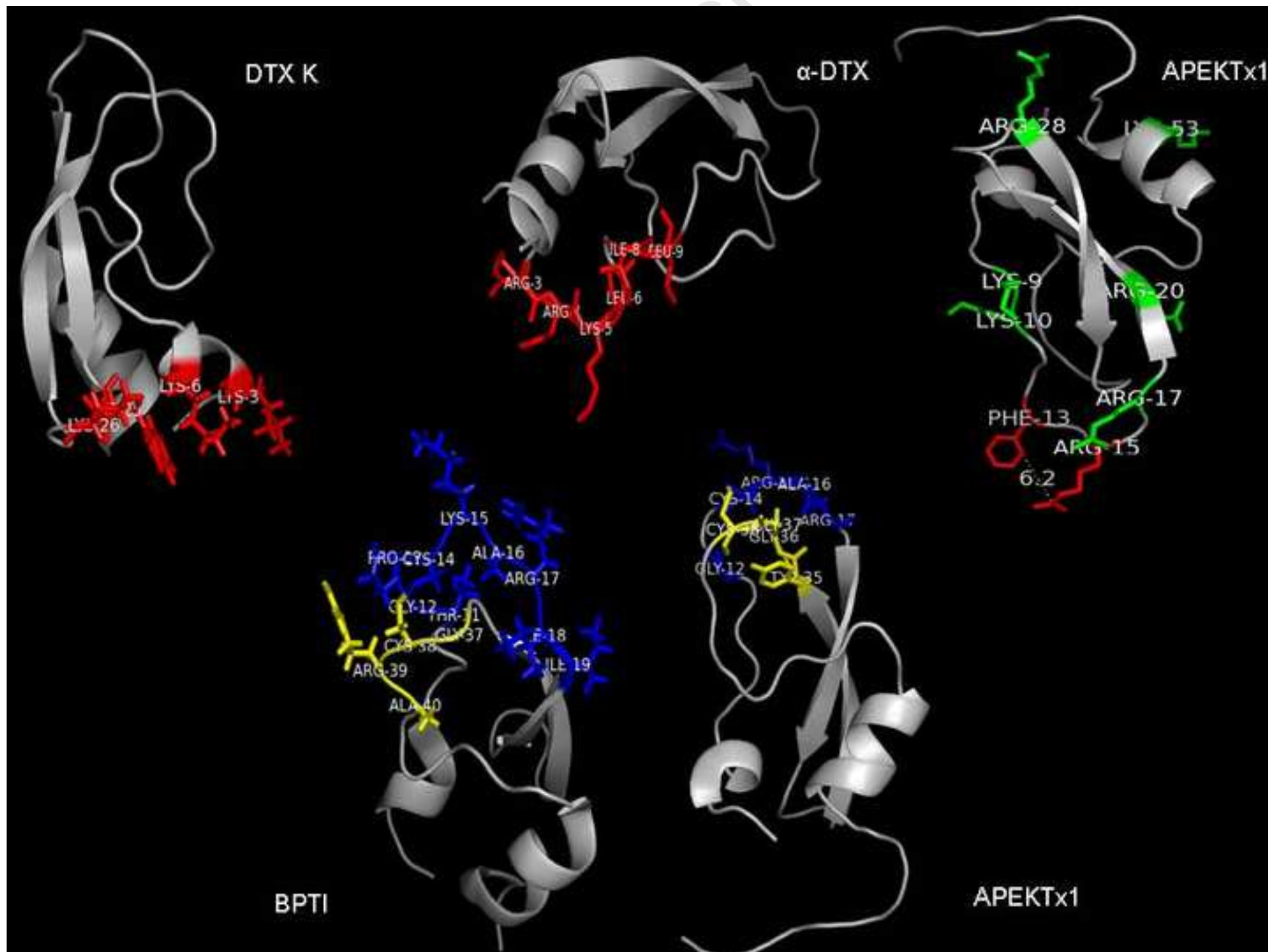
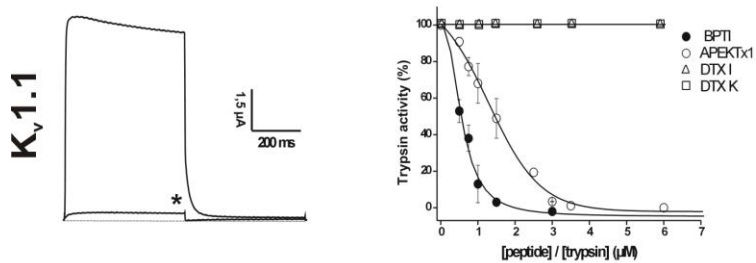




Figure 7



APEKTx1 is a potent and selective  $K_V$  blocker and protease inhibitor



Accepted Manuscript